Nonlinear Dynamics of DNA Chain

Slobodan Zdravković

Deoxyribonucleic acid (DNA) is found in all prokaryotic and eukaryotic cells and many viruses. This complex molecular structure is certainly one of the most interesting molecules. Interest in its structure and dynamics is primarily due to the important role that this molecule plays in life processes. The molecule was first identified in the 1860s by the Swiss chemist Johann Friedrich Miescher. He discovered a substance that had unexpected properties, different from those of the other proteins he had been familiar with. He did not know he had discovered the molecular basis of life, which he called nuclein.

Great progress was made by the German biochemist Albrecht Kossel, who identified the nuclein as a nucleic acid in 1881. He isolated the four nucleotide bases that are the building blocks of DNA, introduced their present names, and obtained the Nobel Prize in 1910.

A revolution has been related to a famous Watson–Crick model, published in a one-page paper [1]. The paper was published in 1953, and the authors were awarded the Nobel Prize in Medicine in 1962. According to the model, DNA is a double helix, formed from two mutually complementary strands, as shown in Fig. 1. We assume that the readers have basic knowledge of its structure [2–7]. It suffices now to point out that each strand represents a series of nucleotides, spaced at $l = 0.34$ nm, whose constituent parts are sugar, phosphate, and base. The nucleotides are always linked together by strong covalent bonds, while different strands interact through basis by weak hydrogen bonds. Adenine (A) is always attached to thymine (T) by two hydrogen bonds, whereas guanine (G) and cytosine (C) are attached by three bonds. This is shown in Fig. 1, where we recognize the two strands representing sugar-phosphate backbones and four kinds of basis. All sugars and phosphates are equal, which means that genetic information depends on the bases only.

S. Zdravković (✉)
Institut za Nuklearne Nauke Vinča, Univerzitet u Beogradu, 11001 Beograd, Serbia
e-mail: szdjidji@vin.bg.ac.rs

S. Zdravković and D. Chevizovich (eds.), *Nonlinear Dynamics of Nanobiophysics*,
https://doi.org/10.1007/978-981-19-5323-1_3

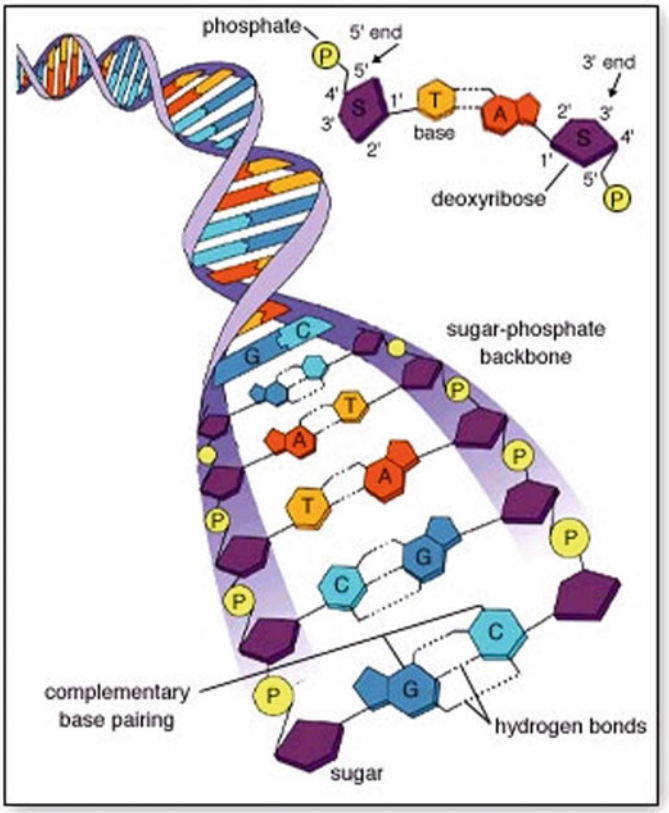

Fig. 1 The structure of DNA molecule

In addition to the H-bonds, the stability of the chain is supported by stacking interactions [5, 8]. These weak forces, interacting between neighbouring bases of the same chain, are of crucial importance for DNA twisting determination.

In conclusion, let us point out that DNA can be seen as a dynamic collection of particles and springs. The particle can be either a nucleotide or any of its constitutive parts. The springs represent chemical bonds. If a certain amount of energy is released at some point, the oscillation of the particles at that point becomes stronger. This affects the neighbouring oscillators, and this transmission is a wave. All this is what we call DNA dynamics.

1 DNA Dynamics

To date, dozens of different mechanical models and their versions have been developed to describe DNA dynamics. For the simplest structural model, the DNA chain is an elastic rod [9]. More advanced models are helical double rod-like models [9]. In both cases, the rods can be either uniform or discrete. According to these simple models, plain waves propagate along the chain.

It was in 1980 when Englander et al. suggested that nonlinear effects might play an important role in DNA dynamics [10]. Instead of the plain waves, the nonlinear effects may focus the vibration energy of DNA into localized soliton-like excitations. Therefore, we can talk about linear and nonlinear models. This is very important to be understood and requires some explanation.

Suppose that there is a strong interaction between two neighbouring particles. An example can be the covalent bond between the nucleotides belonging to the same strand, as explained above. The existence of the strong force means that displacements along the direction of this force are very small. In other words, the oscillations in this direction have small amplitudes. This means that we can assume that attractive and repulsive forces are almost equal and that the corresponding potential energy, or potential for short, should be modelled by a symmetric function. A typical example is the well-known function $f(x) = kx^2/2$. Such a potential is called harmonic, and its usage in science has been called harmonic approximation. Its first derivative represents a force, which is obviously a linear function. On the other hand, if these forces are weak, the corresponding displacements are large and the repulsive and attractive forces are not equal anymore. An example can be the hydrogen bond between the nucleotides belonging to different strands, which was mentioned above. Therefore, to model such potentials, we need non-symmetric functions. A common example is the function $F(x) = D\,[\mathrm{e}^{-a\,x} - 1]^2$, shown in Fig. 2. This potential energy is called the Morse potential. The parameters D and a are the depth and the inverse width of the Morse potential well, respectively. The first derivatives for negative and positive x represent the repulsive and attractive forces, respectively, and it is obvious that the latter one is smaller. For a very large distance between the interacting particles, the first derivative is zero, which means that the particles do not interact anymore. This potential is not harmonic, and its first derivative, i.e., the force, is not a linear function. The models that include at least one anharmonic interaction are called nonlinear. Therefore, the weak interactions are the sources of the nonlinear terms, and, consequently, such systems are nonlinear. As these weak forces are common for biological systems, we concentrate on the nonlinear models only.

Let us explain the first nonlinear model. According to the model, DNA represents two linear chains of pendulums (the bases) connected to the sugar-phosphate backbones, as shown in Fig. 3 [10]. If θ_n is the angle between the pendulum and the direction around which it oscillates, then the total energy is given by the following Hamiltonian

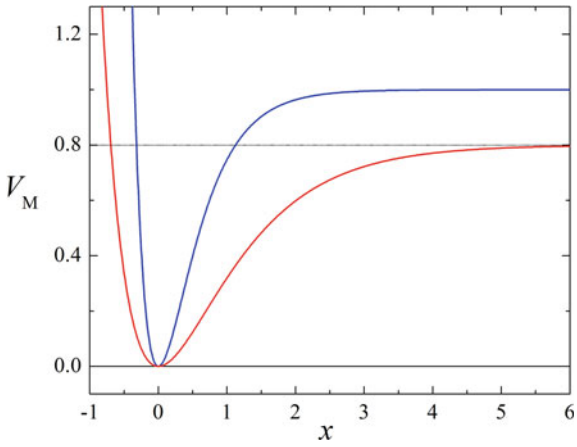

Fig. 2 Morse potential energy $F(x) = D\,[\mathrm{e}^{-a\,x} - 1]^2$ for $D = 1$, $a = 2$ (blue) and $D = 0.8$, $a = 1$ (red)

$$H = \sum \left[\frac{mh^2}{2} \left(\frac{\mathrm{d}\theta_n}{\mathrm{d}t} \right)^2 + \frac{S}{2} (\theta_n - \theta_{n-1})^2 + mgh(1 - \cos\theta_n) \right], \tag{1}$$

where m and h are mass and length of the pendulum, respectively, and S is a harmonic constant, while the number n determines the position of the pendulum [10]. It is clear that nonlinearity is coming from the cosine function.

Using Hamilton's equations and appropriate generalized coordinates, i.e., $\dot{q}_n = \partial H \big/ \partial p_n$, $\dot{p}_n = -\partial H \big/ \partial q_n$, $q_n = \theta_n$, and $p_n = mh^2\dot{\theta}_n$, where the dot means the first derivative with respect to time, the Hamiltonian (1) brings about an appropriate equation of motion, that is

$$mh^2 \left(\frac{\mathrm{d}^2\theta_n}{\mathrm{d}t^2} \right) = S(\theta_{n+1} + \theta_{n-1} - 2\theta_n) - mgh \sin\theta_n. \tag{2}$$

In the static limit, when the term including the second derivative is neglected [10], we obtain the equation

$$S(\theta_{n+1} + \theta_{n-1} - 2\theta_n) - mgh \sin\theta_n = 0, \tag{3}$$

whose solution is

$$\theta_n = 4 \arctan\left[\exp\left(2nl \big/ L\right)\right], \quad L = 2l\sqrt{S \big/ mgh} \tag{4}$$

where l is the distance between two neighbouring pendulums [10]. Its meaning will be clarified in what follows. The function $\theta_n \equiv \theta(n)$ is a kink soliton.

It is convenient, very often, to begin with the discrete case and then pass to the continuum limit $nl \to z$, which will be followed here. The z-axis is in the direction of the DNA chain. This means that when θ_n does not vary too rapidly with n, the

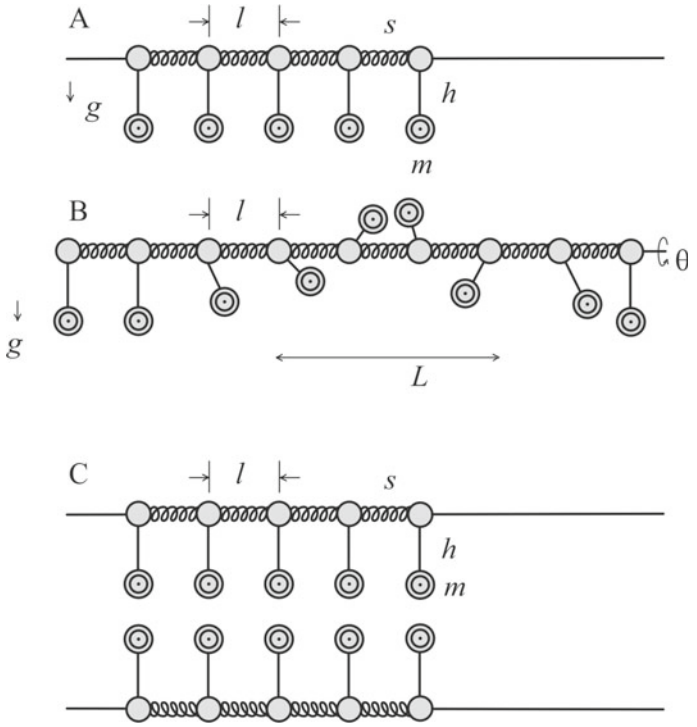

Fig. 3 Mechanical model of the strands of a double helix possessing soliton excitations. Each pendulum is of mass m and length h, spaced at $l = 0.34$ nm along the helix axis. **A** One strand of the duplex capable of undergoing torsional oscillations about the backbone axis in the presence of a restoring force mg. **B** Soliton excitation mode involving a large-amplitude excursion of one pendulum with spreading of the excitation to a group of L. **C** The ground state of the double helix modelled as two linear chains of pendula (the bases) connected by springs (the sugar-phosphate backbones)

following series expansion can be performed:

$$\theta_{n\pm1}(t) \approx \theta(z,t) \pm \theta_z(z,t)l + \frac{1}{2}\theta_{zz}(z,t)l^2, \tag{5}$$

where indices z and zz denote the first and second derivatives with respect to z, respectively, and Eq. (2) becomes

$$mh^2\left(\frac{\partial^2\theta_n}{\partial t^2}\right) - S\left(\frac{\partial^2\theta_n}{\partial z^2}\right) + mgh\sin\theta_n = 0. \tag{6}$$

This is a well-known solvable sine–Gordon equation [11, 12]. Its solutions are the kink and antikink solitons.

Problem 1 Derive Eq. (2).

Problem 2 Plot the function $\theta_n \equiv \theta(n)$, given by Eq. (4), for arbitrary values of the parameters l and L, and convince yourself that this is a kink soliton.

The procedure explained above can be extended, and the DNA molecule can be seen as a series of coupled double pendulums [13, 14]. The first pendulum models the oscillation of the phosphate-sugar part of the nucleotide, while the remaining one describes the oscillation of the base. This approach can be further extended in order to describe inhomogeneous DNA chains [15].

Now, we will explain the Y-model, introduced by Yakushevich in 1989 [16]. According to the model, DNA consists of two parallel chains of discs. The chains are straight, which means that the helicoidal structure is not taken into consideration. The discs are connected to each other with longitudinal and transverse springs. The rigidity of the longitudinal springs is higher than that of the transverse ones as they represent the covalent and hydrogen bonds, respectively. Let us suppose that the chains are in the z-direction, while the surfaces of the discs are in the xy-plane. The model assumes angular oscillations of the discs in the xy-plane only. If $\phi_{i,n}$ represents the angular displacement of the disc, where $i = 1,\ 2$ and $n = 1,\ 2,\ \ldots$ denote the chains and discs, respectively, then the Hamiltonian of DNA is [16]

$$H = \sum_{i,n} \left[\frac{I_i}{2} \phi_{i,n}^2 + \frac{K_i}{2} (\phi_{i,n} - \phi_{i,n-1})^2 + \frac{k}{2} (\Delta l_n)^2 \right]. \tag{7}$$

Here, I_i is the moment of inertia of the discs of the i-th chain, K_i and k are the rigidities of the longitudinal and transverse springs, respectively, and Δl_n is the stretching of the n-th transverse spring due to rotations of the discs. Let us determine Δl_n first. Imagine two discs of the radius R in the common plain at the position n. Then, the distance between their centres is $2R + l_0$, where l_0 is nothing but the length of the unstretched spring. This is shown in Fig. 4. Suppose that these two discs perform the angular displacements $\phi_{1,n}$ and $\phi_{2,n}$. These angles are denoted by ϕ_1 and ϕ_2 in Fig. 4 for short. The new length becomes l_n, where

$$l_n^2 = \left(l_0 + 2R - R\cos\phi_{1,n} - R\cos\phi_{2,n}\right)^2 + \left(R\sin\phi_{1,n} - R\sin\phi_{2,n}\right)^2, \tag{8}$$

and, consequently,

$$\Delta l_n = l_n - l_0. \tag{9}$$

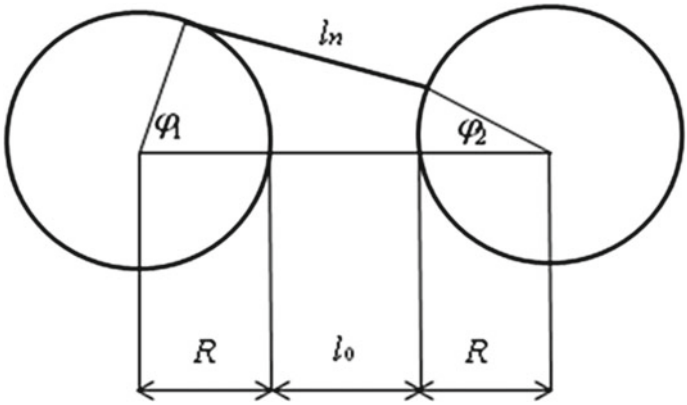

Fig. 4 Cross-section of the model consisting of two strands

Problem 3 Derive Eq. (8).

Using the Hamilton's equations and the generalized coordinates $q_i = \phi_i$ and $p_i = I_i\dot{\phi}_i$, we easily obtain the dynamical equations of motion according to Eqs. (7)–(9). The one for $\phi_{1,n}$ is

$$I_1\ddot{\phi}_{1,n} = K_1\left(\phi_{1,n+1} + \phi_{1,n-1} - 2\phi_{1,n}\right)^2 - k\frac{\Delta l_n}{l_n}\left[\left(2R^2 + Rl_0\right)\sin\phi_{1,n}\,,\right.$$
$$\left. -R^2\sin\left(\phi_{1,n} + \phi_{2,n}\right)\right] \tag{10}$$

while the remaining equation can be obtained from Eq. (10) by replacing the index 1 by 2.

Problem 4 Derive Eq. (10).

The next step is the continuum limit. This means that we replace $\phi_{i,n}(t)$ with $\phi_i(z,t)$, where the coordinate z is in the direction of the chains, as explained above. This simplifies Eq. (10), and we straightforwardly obtain

$$I_1\ddot{\phi}_1 = K_1a^2\phi_{1zz} - k\frac{\Delta l}{l}\left[\left(2R^2 + Rl_0\right)\sin\phi_1 - R^2\sin(\phi_1 + \phi_2)\right], \tag{11}$$

as well as the corresponding one for $\phi_1 \leftrightarrow \phi_2$. Notice that $\Delta l\big/l$ depends on the functions ϕ_1 and ϕ_2, which means that Eq. (11) is very far from being solvable. Fortunately, we can assume $l_0 << R$, which suggests a new approximation $l_0 \approx 0$

[16], yielding to $\Delta l/l = 1$ in Eq. (11). All this brings about the following system of equations

$$\left.\begin{aligned} I_1\ddot{\phi}_1 &= K_1a^2\phi_{1zz} - kR^2[2\sin\phi_1 - \sin(\phi_1+\phi_2)],\\ I_2\ddot{\phi}_2 &= K_2a^2\phi_{2zz} - kR^2[2\sin\phi_2 - \sin(\phi_1+\phi_2)] \end{aligned}\right\}. \tag{12}$$

This system is nonintegrable in general. In the case of linear approximation, i.e., for very small oscillations, the solutions for ϕ_1 and ϕ_2 are plain waves, as expected. For $\varphi_1 = -\varphi_2$ and $\varphi_1 = \varphi_2$, Eq. (12) reduces to the sine–Gordon and double sine–Gordon equations, respectively. These particular equations have one feature in common: they have soliton-like solutions named kinks and antikinks. So, we can expect that the system (12) might also have soliton-like solutions of kink and antikink types [16].

Y-model has been subjected to a variety of improvements. For example, the helicoidal structure of DNA was taken into consideration in [17], while in [18], it was not assumed that all bases are equal and, consequently, a more realistic model was explained. In [19], the author did not assume the approximation $l_0 \approx 0$, while Morse potential was introduced in [20] to model the weak hydrogen bonds. Of special importance is the composite Y-model [21]. A key point is that the sugar-phosphate group and base are described by separate degrees of freedom. The composite Y-model contains the Y-model as a particular case. It represents an improvement providing a more realistic description of DNA. We should point out that the existence of solitons is a generic feature of the underlying nonlinear dynamics and is to a large extent independent of the detailed modelling of DNA [21]. Finally, let us point out that the Y-model allows us to study DNA dynamics under external influences [20, 22, 23].

A key problem in each model is the choice of degrees of freedom. Namely, DNA dynamics can be connected with either an angular or radial displacements of the bases from their equilibrium positions. The latter ones will be explained in what follows. This means that if we assume only one degree of freedom per nucleotide, we can choose either angular or radial variable as the coordinate, and the appropriate models can be called angular (torsional) and radial models, respectively. Of course, some extensions, i.e., models combining both kinds of coordinates, are possible [24–29]. The models mentioned above [10, 16, 21] are obviously the angular ones. In what follows, we describe a couple of radial models. We start with the Peyrard–Bishop (PB) model and further describe its two improvements, which we call the helicoidal Peyrard–Bishop (HPB) and Peyrard–Bishop–Dauxois (PBD) models.

To understand the PB model, we should remind ourselves of the chemical bonds existing between the nucleotides within DNA. In Fig. 5, we recognize the two strands. The interactions between the nucleotides belonging to the same strand are very strong, and the corresponding oscillations are negligible. On the other hand, the bases of the nucleotides belonging to the different strands interact through weak hydrogen bonds, modelled by the Morse potential, as explained above. Hence, these oscillations are not negligible, and it certainly makes sense to choose the radial displacements u_n

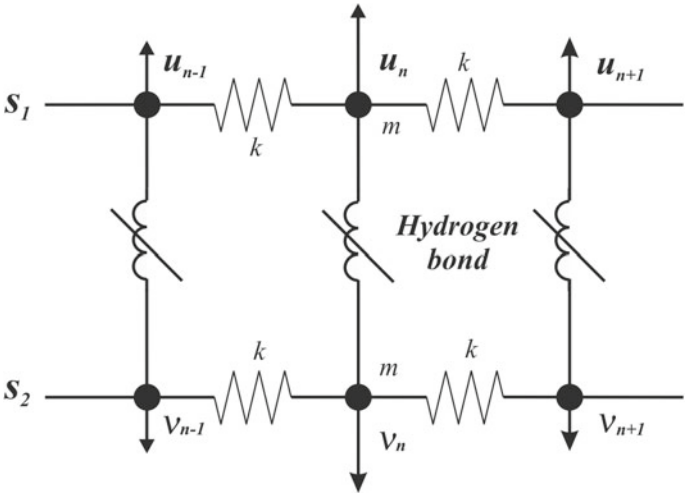

Fig. 5 A simplified structure of DNA molecule

and v_n as the crucial degrees of freedom. Notice that the strands are linear systems, while DNA, due to the weak interactions, is not.

Like above, we start with the discrete Hamiltonian and pass to the continuum limit. According to the PB model, the Hamiltonian for DNA, in the nearest neighbour approximation, is [30, 31]

$$H = \sum \left\{ \frac{m}{2}\left(\dot{u}_n^2 + \dot{v}_n^2\right) + \frac{k}{2}\left[(u_n - u_{n-1})^2 + (v_n - v_{n-1})^2\right] + D\left[\mathrm{e}^{-a(u_n - v_n)} - 1\right]^2 \right\}, \tag{13}$$

where $m = 300$ amu $= 5.1 \times 10^{-25}$ kg is the nucleotide mass, k is a constant of the harmonic interaction, and $\dot{u}_n$ and $\dot{v}_n$ represent the appropriate velocities. Obviously, the coordinates u_n and v_n are longitudinal (radial) displacements of the nucleotides at the position n from their equilibrium positions along the direction of the hydrogen bond. One can recognize the kinetic energy term, potential energy describing the covalent interaction, and the Morse potential.

It is convenient to introduce new coordinates representing the in-phase and out-of-phase transversal motions as

$$x_n = (u_n + v_n)/\sqrt{2}, \quad y_n = (u_n - v_n)/\sqrt{2}, \tag{14}$$

which transforms Hamiltonian (13) into

$$H = \sum \left\{ \frac{m}{2}(\dot{x}_n^2 + \dot{y}_n^2) + \frac{k}{2}\left[(x_n - x_{n-1})^2 + (y_n - y_{n-1})^2\right] + D\left[e^{-a\sqrt{2}y_n} - 1\right]^2 \right\}. \tag{15}$$

Therefore, the coordinate x_n describes the oscillation of the centre of mass, while y_n is proportional to the stretching of the nucleotide pair at position n. We are going to see that the function $x_n(t)$ represents a linear wave, while $y_n(t)$ is a nonlinear one and, consequently, more interesting for us. It is important to know that $y_n(t)$ is not temperature-dependent, but its mean value $\langle y \rangle$ is [30–32]. We do not explain the model in detail as this will be done through one of its improved versions. In fact, the PB model is a special case of the HPB one.

The PB model does not take helicoidal DNA structure into consideration, while its improved version, the HPB model, does. This has been achieved by introducing an additional term, describing helicoidal interactions, into Eq. (15), and the Hamiltonian becomes [33]

$$\begin{aligned} H = \sum \Bigg\{ & \frac{m}{2}\left(\dot{u}_n^2 + \dot{v}_n^2\right) + \frac{k}{2}\left[(u_n - u_{n-1})^2 + (v_n - v_{n-1})^2\right] \\ & + \frac{K}{2}\left[(u_n - v_{n+h})^2 + (u_n - v_{n-h})^2\right] + D\left[\mathrm{e}^{-a(u_n - v_n)} - 1\right]^2 \Bigg\} \end{aligned} \tag{16}$$

where K is the harmonic constant of the helicoidal spring. To understand the new helicoidal term, we should imagine DNA in Fig. 5 being twisted. This means that after a turn of π, the nucleotide belonging to one strand at the position n will be close to both the $(n + h)$th and $(n - h)$th nucleotides of the other strand [33]. As the helix has a helical pitch of about 10 base pairs per turn [34], one can assume $h = 5$. Of course, we use Eq. (14) again, as well as the generalized coordinates $q_{nx} = x_n, q_{ny} = y_n, p_{nx} = m\dot{x}_n$, and $p_{ny} = m\dot{y}_n$, and obtain the following completely decoupled dynamical equations of motion

$$m\ddot{x}_n = k(x_{n+1} + x_{n-1} - 2x_n) + K(x_{n+h} + x_{n-h} - 2x_n) \tag{17}$$

$$\begin{aligned} m\ddot{y}_n = {} & k(y_{n+1} + y_{n-1} - 2y_n) - K(y_{n+h} + y_{n-h} + 2y_n) \\ & + 2\sqrt{2}aD\left(\mathrm{e}^{-a\sqrt{2}y_n} - 1\right)\mathrm{e}^{-a\sqrt{2}y_n} \end{aligned} \tag{18}$$

Problem 5 Derive Eqs. (17) and (18).

In the continuum limit, i.e., if we apply Eq. (5), both terms in the brackets in Eq. (17) will transform into the second derivatives with respect to the spatial coordinate. This means that we obtain an ordinary wave equation whose solution is the usual

linear wave (phonon). However, Eq. (18) describes a nonlinear wave. We restrict our attention to it and assume that the oscillations of nucleotides are large enough to be anharmonic but still small enough so that the nucleotides oscillate around the bottom of the Morse potential well. This suggests the transformation

$$y_n = \varepsilon\, \Phi_n; \qquad (\varepsilon \ll 1) \tag{19}$$

and Eq. (18) becomes

$$\begin{aligned} \ddot{\Phi}_n = {} & \frac{k}{m}\,(\Phi_{n+1} + \Phi_{n-1} - 2\Phi_n) - \frac{K}{m}\,(\Phi_{n+h} + \Phi_{n-h} + 2\Phi_n) \\ & - \omega_g^2\big(\Phi_n + \varepsilon\,\alpha\,\Phi_n^2 + \varepsilon^2\beta\,\Phi_n^3\big), \end{aligned} \tag{20}$$

where

$$\omega_g^2 = \frac{4a^2 D}{m}\,, \quad \alpha = \frac{-3a}{\sqrt{2}} \text{ and } \beta = \frac{7a^2}{3} \tag{21}$$

Problem 6 Derive Eq. (20).

Now, we solve Eq. (20) following [7], where all the derivations can be found. To solve it, we use a semi-discrete approximation, which means that we look for the wave solutions of the form

$$\Phi_n(t) = F_1(\xi)\mathrm{e}^{i\theta_n} + \varepsilon\left[F_0(\xi) + F_2(\xi)\,\mathrm{e}^{i2\theta_n}\right] + \mathrm{cc} + \mathrm{O}\big(\varepsilon^2\big) \tag{22}$$

$$\xi = (\varepsilon\, nl, \varepsilon\, t), \quad \theta_n = nql - \omega t \tag{23}$$

where $l = 0.34\mathrm{nm}$ is the distance between two neighbouring nucleotides in the same strand, ω is the optical frequency of the linear approximation, $q = 2\pi \big/ \lambda$ is the wavenumber, cc represents complex conjugate terms, and the function F_0 is real. This is a modulated wave where F_1 is a continuous function representing the envelope, while the carrier component $\mathrm{e}^{i\theta_n}$ is discrete. As the frequency of the carrier wave is much higher than the frequency of the envelope, we need the two time scales, t and $\varepsilon\, t$, for those two functions, which can be seen in Eq. (23). Of course, the same holds for the coordinate scales. A mathematical basis for this procedure is the multiple-scale method or the derivative-expansion method [35, 36].

From Eq. (22), one can see the true meaning of the parameter ε. The higher-order terms are required because of the last two terms in Eq. (20).

Now, we switch to the continuum limit $nl \to z$ and use the transformations

$$Z = \varepsilon z; \quad T = \varepsilon t, \tag{24}$$

which yield

$$\begin{aligned}\Phi_n(t) \to\ & F_1(Z,T)\mathrm{e}^{i\theta} + \varepsilon\left[F_0(Z,T) + F_2(Z,T)\mathrm{e}^{i2\theta}\right] + \mathrm{cc} \\ =\ & F_1\mathrm{e}^{i\theta} + \varepsilon\left[F_0 + F_2\mathrm{e}^{i2\theta}\right] + F_1^*\mathrm{e}^{-i\theta} + \varepsilon F_2^*\mathrm{e}^{-i2\theta}\end{aligned} \tag{25}$$

where the star stands for complex conjugate and $F_i \equiv F_i(Z,T)$. Also, a very important relation is

$$F_i(\varepsilon(n \pm h)l, \varepsilon t) \to F_i(Z,T) \pm F_{i\,Z}(Z,T)\varepsilon l h + \frac{1}{2}F_{i\,ZZ}(Z,T)\,\varepsilon^2 l^2 h^2, \tag{26}$$

where index Z denotes differentiation with respect to the coordinate Z [7]. All this enables us to determine the expressions existing in Eq. (20), such as

$$\begin{aligned}\Phi_{n+h} + \Phi_{n-h} + 2\Phi_n = \{&2F_1\left[\cos(qhl) + 1\right] + 2i\varepsilon hl F_{1Z}\sin(qhl) \\ &+\varepsilon^2 h^2 l^2 F_{1ZZ}\cos(qhl)\Big\}\mathrm{e}^{i\theta} \\ &+ \left\{2\varepsilon F_2\left[\cos(2qhl) + 1\right] + 2i\varepsilon^2 hl F_{2Z}\sin(2qhl)\right\}\mathrm{e}^{i2\theta} \\ &+ 4\varepsilon F_0 + \mathrm{cc},\end{aligned} \tag{27}$$

$$\dot{\Phi}_n = \varepsilon\, F_{1T}e^{i\theta} - i\omega F_1\mathrm{e}^{i\theta} + \varepsilon^2 F_{0T} + \varepsilon^2 F_{2T}\mathrm{e}^{i2\theta} - 2i\varepsilon\omega F_2\mathrm{e}^{i2\theta} + \mathrm{cc}, \tag{28}$$

and

$$\Phi_n^3 = 3|F_1|^2 F_1\,\mathrm{e}^{i\theta} + 3|F_1|^2 F_1^*\,\mathrm{e}^{-i\theta} + F_1^3\mathrm{e}^{i3\theta} + F_1^{*3}\mathrm{e}^{-i3\theta} + \mathrm{O}(\varepsilon). \tag{29}$$

Finally, we obtain the continuum version of Eq. (20), that is,

$$\begin{aligned}&(\varepsilon^2 F_{1TT} - 2i\varepsilon\omega F_{1T} - \omega^2 F_1)\,\mathrm{e}^{i\theta} - (4i\varepsilon^2\omega F_{2T} + 4\varepsilon\omega^2 F_2)\,\mathrm{e}^{i2\theta} + \mathrm{cc} \\ &= \frac{k}{m}\{2F_1\left[\cos(ql) - 1\right]\mathrm{e}^{i\theta} + 2i\varepsilon l F_{1Z}\sin(ql)\,\mathrm{e}^{i\theta} + \varepsilon^2 l^2 F_{1ZZ}\cos(ql)\,\mathrm{e}^{i\theta} \\ &+2\varepsilon F_2[\cos(2ql) - 1]\,\mathrm{e}^{i2\theta} + 2i\varepsilon^2 l F_{2Z}\sin(2ql)\,\mathrm{e}^{i2\theta} + \mathrm{cc}\Big\} \\ &-\frac{K}{m}\{2F_1[\cos(qhl) + 1]\,\mathrm{e}^{i\theta} + 2i\varepsilon hl F_{1Z}\sin(qhl)\,\mathrm{e}^{i\theta} + \varepsilon^2 h^2 l^2 F_{1ZZ}\cos(qhl)\,\mathrm{e}^{i\theta} \\ &+2\varepsilon F_2[\cos(2qhl) + 1]\,\mathrm{e}^{i2\theta} + 2i\varepsilon^2 hl F_{2Z}\sin(2qhl)\,\mathrm{e}^{i2\theta} + 4\varepsilon F_0 + \mathrm{cc}\Big\} \\ &-\omega_g^2\left[F_1\,\mathrm{e}^{i\theta} + \varepsilon F_0 + \varepsilon F_2\,\mathrm{e}^{i2\theta} + 2\varepsilon\alpha|F_1|^2 + 2\varepsilon^2\alpha(F_0F_1 + F_1^*F_2)\,\mathrm{e}^{i\theta}\right. \\ &\left.+\varepsilon\alpha F_1^2\,\mathrm{e}^{i2\theta} + 2\varepsilon^2\alpha F_1F_2\,\mathrm{e}^{i3\theta} + 3\varepsilon^2\beta|F_1|^2F_1\,\mathrm{e}^{i\theta} + \varepsilon^2\beta F_1^3\,\mathrm{e}^{i3\theta} + \mathrm{cc}\right]\end{aligned} \tag{30}$$

Problem 7 Derive Eq. (27).

Problem 8 Derive Eq. (30). Hint: Derive the expressions for $\dot{\Phi}_n$, Φ_n^2, and $\Phi_{n+1} + \Phi_{n-1} - 2\Phi_n$ first.

Let us keep in mind that we are looking for the solution $\Phi_n(t)$. The crucial expression (30) enables us to obtain the functions $F_1(\xi)$, $F_0(\xi)$, and $F_2(\xi)$, required for the determination of $\Phi_n(t)$, as clear from Eq. (22). To do this, we should equate the coefficients for the various harmonics [6, 7, 33]. Thus, the coefficients for $e^{i\theta}$ give

$$\begin{aligned}\varepsilon^2 F_{1TT} - 2i\varepsilon\omega F_{1T} - \omega^2 F_1 = \frac{k}{m}[2F_1(\cos(ql) - 1) \\ +2i\varepsilon l F_{1Z}\sin(ql) + \varepsilon^2 l^2 F_{1ZZ}\cos(ql)\big] \\ -\frac{K}{m}[2F_1(\cos(qhl) + 1) + 2i\varepsilon hl F_{1Z}\sin(qhl) \\ +\varepsilon^2 h^2 l^2 F_{1ZZ}\cos(qhl)\big] \\ -\omega_g^2\big[F_1 + 2\varepsilon^2\alpha F_0 F_1 + 2\varepsilon^2\alpha F_1^* F_2 + 3\varepsilon^2\beta|F_1|^2 F_1\big]\end{aligned} \tag{31}$$

Neglecting all the terms with ε and ε^2, we get the dispersion relation

$$\omega^2 \equiv \omega_y^2 \equiv \omega_o^2 = \big(4/m\big)\left[a^2 D + k\sin^2\big(ql/2\big) + K\cos^2\big(qhl/2\big)\right], \tag{32}$$

which brings about the expression for the group velocity $d\omega/dq$ as

$$V_g = \frac{l}{m\omega}\left[k\sin(ql) - Kh\sin(qhl)\right] \tag{33}$$

The corresponding dispersion relation for the in-phase oscillations described by Eq. (17) is

$$\omega_x^2 \equiv \omega_a^2 = \big(4/m\big)\left[k\sin^2\big(ql/2\big) + K\sin^2\big(qhl/2\big)\right]. \tag{34}$$

The frequencies ω_y and ω_x are usually called optical and acoustical, respectively.

Problem 9 Derive Eqs. (31) and (32).

Problem 10 Derive Eq. (34).

Problem 11 Plot the functions $\omega_o(ql)$ and $\omega_a(ql)$. Compare these two functions for different values of the parameters K and $a^2 D$.

Equating the coefficients for $e^{i0} = 1$ in Eq. (30), we straightforwardly obtain

$$F_0 = \mu\,|F_1|^2; \quad \mu = -2\alpha\left(1 + \frac{4K}{m\omega_g^2}\right)^{-1} \tag{35}$$

while $e^{i2\theta}$ gives

$$F_2 = \delta\,F_1^2; \delta = \omega_g^2\,\alpha\left[4\omega^2 - \frac{4k}{m}\,\sin^2(ql) - \frac{4K}{m}\cos^2(hql) - \omega_g^2\right]^{-1} \tag{36}$$

Problem 12 Derive Eq. (36).

As the functions F_0 and F_2 can be expressed through F_1, the equation for F_1 should be derived. We use the new coordinates

$$S = Z - V_g\,T, \quad \tau = \varepsilon\,T, \tag{37}$$

again and obtain the transformations for F_{1Z}, F_{1ZZ}, F_{1T}, and F_{1TT} existing in Eq. (30). We notice that ε exists in the time coordinate but does not in the space one. This definition ensures that the time variation of the envelope of the function F_1, in units of $1/\omega$, be smaller than its spatial variation in units of l [37]. Finally, using Eqs. (31)–(33) and (35)–(37), we easily obtain the well-known nonlinear Schrödinger equation (NLSE) for the function F_1

$$i\,F_{1\tau} + P\,F_{1SS} + Q\,|F_1|^2 F_1 = 0, \tag{38}$$

where the dispersion coefficient P and the coefficient of nonlinearity Q are given by

$$P = \frac{1}{2\omega}\left\{\frac{l^2}{m}\left[k\cos(ql) - K\,h^2\cos(qhl)\right] - V_g^2\right\}, Q = -\frac{\omega_g^2}{2\omega}\left[2\alpha\,(\mu + \delta) + 3\beta\right] \tag{39}$$

Problem 13 Derive Eqs. (38) and (39).

This is a solvable equation, and its analytical solution, for $PQ > 0$, is [33, 38, 39]

$$F_1(S,\tau) = A_0 \operatorname{sech}\left(\frac{S-u_e\tau}{L_e}\right)\exp\frac{iu_e(S-u_c\tau)}{2P}, \quad u_e > 2u_c \cdot u_e > 2u_c. \tag{40}$$

Here, we assume $P > 0$ and $Q > 0$ [38]. The values for the envelope amplitude A_0 and its width L_e will be written later. The function (40) is obviously the modulated solitary wave, where u_e and u_c are the velocities of the envelope and carrier waves, respectively.

Problem 14 Make sure that Eq. (40) satisfies Eq. (38). Show that $A_0 = \sqrt{\frac{u_e^2-2u_eu_c}{2PQ}}$ and $L_e = \frac{2P}{\sqrt{u_e^2-2u_eu_c}}$.

Therefore, we have obtained the expression for F_1, the functions F_0 and F_2 can be expressed through F_1, and, according to Eqs. (19), (22), and (23), we can easily reach our final goal, which is the function $y_n(t)$.

However, before we proceed, we need to comment on a couple of the parameters existing in the HPB model. Some of them have appeared in the Hamiltonian (16). They are so-called intrinsic parameters, describing the geometry and the chemical interactions within DNA. However, there are parameters coming from the applied mathematical procedure. Let us concentrate on the mathematical parameters u_e, u_c, and ε. The velocities u_e and u_c are included in the solution of the NLSE, while ε does not have any physical meaning. This only helps us to distinguish big and small terms in the series expansion (22). A careful investigation of all the formulae shows that only two mathematical parameters are relevant and they are εu_e and εu_c. Also, it is very difficult to pick the appropriate values for u_e and u_c according to the requirement $u_e > 2u_c$ only. However, the ratio of these speeds belongs to the interval [0;0.5), which is much more convenient to deal with. Hence, we choose the following two mathematical parameters [40]

$$U_e = \varepsilon u_e, \quad \eta = \frac{u_c}{u_e}, \quad 0 \le \eta < 0.5 \tag{41}$$

We will return to this point later and show how U_e can be expressed through η.

Finally, according to Eqs. (19), (22)–(24), (35), (36), (38), and (41), the stretching of the nucleotide pair at the position n, i.e., the solution of Eq. (18), is

$$y_n(t) = 2A\text{sech}\left(\frac{nl - V_e t}{L}\right)\{\cos(\Theta nl - \Omega t) + A\text{sech}\left(\frac{nl - V_e t}{L}\right)\left[\frac{\mu}{2} + \delta\cos(2(\Theta nl - \Omega t))\right]\} \tag{42}$$

where

$$A \equiv \varepsilon A_0 = |U_e|\sqrt{\frac{1-2\eta}{2PQ}}, \quad L \equiv \frac{L_e}{\varepsilon} = \frac{2P}{|U_e|\sqrt{1-2\eta}}. \tag{43}$$

The envelope velocity V_e, wavenumber Θ, and frequency Ω are given by

$$V_e = V_g + U_e, \quad \Theta = q + \frac{U_e}{2P}, \quad \Omega = \omega + \frac{(\mathrm{V}_g + \eta U_e)\, U_e}{2P} \tag{44}$$

Problem 15 Derive Eqs. (42)–(44).

To plot the function $y_n(t)$, the values of all the parameters should be known. The problem with the mathematical parameter U_e can be solved by assuming that the most favourable mode is a coherent one (CM), according to which the envelope and the carrier wave velocities are equal, i.e., [41]

$$V_e = \frac{\Omega}{\Theta}. \tag{45}$$

This means that the function $y_n(t)$ is the same at any position n. In other words, the wave preserves its shape in time, indicating high stability [40].

Problem 16 To better understand the previous statement, plot the modulated wave $f(x) = \text{sec h(x - ct)}\cos[10(\text{x} - \text{t})]$ for different t for the two cases: (a) $c = 1$ (CM) and (b) $c \neq 1$.

Notice that the requirement (45) ensures that Eq. (42) becomes a one-phase function. This means that $y_n(t)$ depends on nl and t through $\zeta = nl - V_e t$, where V_e is a constant, representing the travelling wave velocity. If a solitary wave, or soliton for short, is defined as a localized travelling wave [39], then $y_n(t)$, obviously being localized, satisfies the requirements for being the soliton. In other words, the CM is nothing but the solitonic mode (SM) [7]. According to Eq. (45), one can easily obtain the function $U_e(\eta)$, which is

$$U_e = \frac{P}{1-\eta}\left[-q + q\sqrt{1 + \frac{2(1-\eta)}{Pq^2}(\omega - qV_g)}\right]. \tag{46}$$

This is a slowly increasing function of η [40].

Problem 17 Derive Eq. (46).

Notice that no experimental evidence that CM is the most favourable one, as suggested above, exists. This is still an open question, one of many open questions in DNA dynamics, requiring further research. One of the future research directions could be to study the stability of the solution (42) for different cases, i.e., for $V_e > \frac{\Omega}{\Theta}$, $V_e = \frac{\Omega}{\Theta}$, and $V_e < \frac{\Omega}{\Theta}$. Also, it is important to keep in mind that Eq. (20) is a discrete one. To obtain the solution (42), this equation was subjected to the semi-discrete approximation, as explained above. One important future task should be to numerically solve Eq. (20) for all three relationships between V_e and Ω/Θ. This will shed new light on the question regarding the most favourable mode.

In what follows, we assume CM, i.e., Eq. (46). This means that we have solved the problem regarding the parameter U_e. Let us study η now. It was pointed out that Eq. (42) represents the modulated wave. It is useful to define a certain physical quantity, which determines the efficiency of the modulation. This can be a density of internal oscillations (density of carrier wave oscillations) [41]. This is a ratio of the wavenumbers of the wave components or a ratio of the appropriate periods. According to Eq. (42), we can define the wavelengths and periods of both the envelope and carrier wave as

$$\frac{2\pi}{\Lambda} = \frac{1}{L}, \quad \frac{2\pi}{\Lambda_c} = \Theta, \quad \frac{2\pi}{T} = \frac{V_e}{L}, \frac{2\pi}{T_c} = \Omega, \tag{47}$$

where the index c denotes the carrier component. Then, we define the density in two ways, that is,

$$D_o \equiv \frac{\Lambda}{\Lambda_c} = L\Theta, \quad \Gamma_o \equiv \frac{T}{T_c} = \frac{L\Omega}{V_e} \tag{48}$$

They are equal as they should be if Eq. (45) is satisfied. This is strong support for the CM. In what follows, we plot $D_o(\eta)$, as well as $A_m(\eta) = 2A$, and try to pick an acceptable value for the parameter η. However, to do these plots, we should know, or assume, the values of the remaining intrinsic parameters. They are k, K, a, and D, existing in Eq. (16), and q, which has appeared in Eq. (23). The experimental values of these parameters do not exist, and this has turned out to be a very tough problem. It is very likely that the most detailed analysis has been performed in [42]. It was shown that there are a couple of requirements that should be satisfied. In this chapter, we use the following set of parameters, to satisfy all these requirements [7,

42]:

$$a = 1.2\ \mathring{\text{A}}^{-1}, \quad D = 0.07\ \text{eV}, \quad k = 12\ \text{N/m}, \quad K = 0.08\ \text{N/m}, \quad ql = 2\pi/10. \tag{49}$$

Let us remember that $q = 2\pi \big/ \lambda$ is the wavenumber. For $\lambda = Nl$, where N is a number, not necessarily an integer, one obtains $ql = 2\pi \big/ N$. Therefore, $N = 10$ has been assumed in Eq. (49).

Problem 18 Show that $D_\text{o} = \Gamma_\text{o}$ if Eq. (46) holds.

Now, we can plot the functions $D_\text{o}(\eta)$ and $A_m(\eta)$. They are shown in Figs. 6 and 7, respectively. The plots were done according to Eqs. (21), (32), (33), (35), (36), (39), (43), (44), (46), (48), and (49). We see that, for very small η, modulation, practically, does not exist. If we assume that modulation represents a key factor in DNA dynamics, then it is very likely that Γ_o cannot be less than 6. This means that η should not be smaller than 0.45. Figure 7 also shows that the small values for η are not acceptable. If we expect that A_m cannot be bigger than $0.3\ \mathring{\text{A}}$, we come up with the same conclusion as above. Notice that $A_m = 2A$ is not real amplitude. From Eq. (42), we see that $y_n(t)$ has maximal value y_m when the cosine and secant hyperbolic functions are equal to one. Such a curve is similar to one depicted in Fig. 7 but is roughly 1.5 times bigger. For example, the starting point for $\eta = 0$ would be 0.97 instead of 0.63 shown in Fig. 7. As a conclusion, in what follows, we use $\eta = 0.47$.

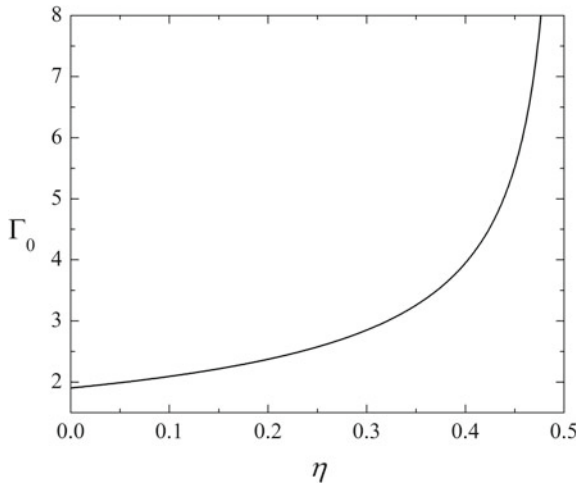

Fig. 6 Density of internal oscillations Γ_o as a function of the parameter η

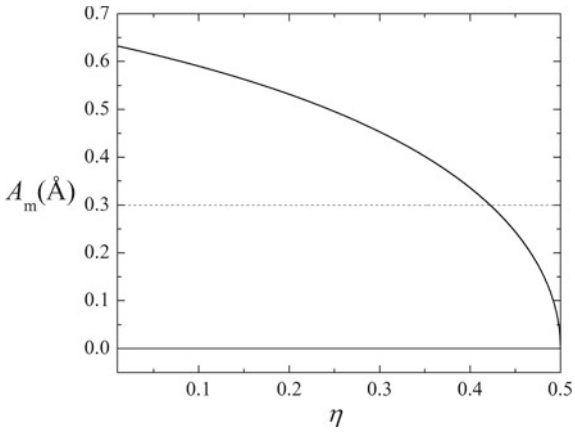

Fig. 7 Amplitude $A_m = 2A$ as a function of the parameter η

Problem 19 Make sure that U_e, given by Eq. (46), is real for the values of the parameter existing in Eq. (49) and for $\eta = 0.47$.

Problem 20 Plot the real maximum of $y_m(\eta)$ and verify the statements from the previous paragraph.

Finally, we can plot the nucleotide pair stretching as a function of the position, i.e., the function $y_n(t)$. This is depicted in Fig. 8 as a function of the position for a particular time t.

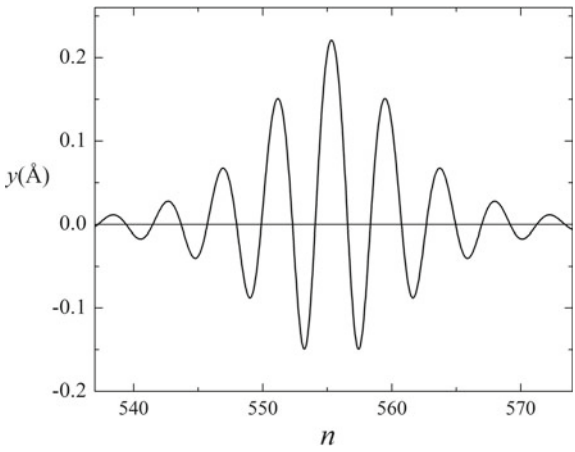

Fig. 8 Nucleotide pair stretching at $t = 100$ ps for: $a = 1.2\ \mathring{\text{A}}^{-1}$, $D = 0.07$ eV, $k = 12$ N/m, $K = 0.08$ N/m, $ql = 2\pi/10$, and $\eta = 0.47$

Problem 21

(a) Plot Fig. 8 for at least two different values of t. Make sure that the shape of the curve has not been changed for the different t.
(b) Do the same for the non-coherent mode. Hint: Calculate U_e according to Eq. (46) and pick another value to do the required plot.

Problem 22 Calculate y_m, U_e, Λ, V_g, and U_e for the values of the parameters used for Fig. 8. (Solutions: $\Gamma_o = 7.1$, $\Lambda = 30.2\,l$, $V_g = 1011$ m/s, and $U_e = 877$ m/s).

It is obvious that this is a localized modulated wave, usually called a breather. If we had picked a different time, we would have obtained exactly the same shape of the wave but at a different position. This is so because the CM was assumed. Also, we could have assumed a certain position and plotted $y_n(t)$ as a function of time.

According to Fig. 8, one can see that the positive amplitude is a little bit bigger than the negative one. This comes from the higher-order terms in Eqs. (22) and (42). Basically, this is a result of the fact that the Morse potential is not symmetric, which means that the repulsive force between the nucleotides is stronger than the attractive one.

Based on Fig. 8, we can conclude that the soliton covers about 30 nucleotide pairs. In other words, the wavelength, defined by Eq. (47), is $\Lambda = 30.2\,l$. Unfortunately, appropriate experimental values do not exist. However, this width can be compared with the solitonic width at a DNA segment involved in a process of transcription [7]. It was reported [43] that this width is between 8 and 17 nucleotides, while some experimental works suggest that this segment covers between 7 and 15 base pairs [44]. The width shown in Fig. 8 is higher, but we should keep in mind that the transcription is followed by a local unzipping, which can be understood as an extremely high amplitude. The wave shown in Fig. 8 is an "ordinary" one, while the solitons at the mentioned segments have much higher amplitudes, corresponding to the local unzipping, which is a topic of the next sections. As the increase of the amplitude means the decrease of the solitonic width, we can conclude that the solitonic width, corresponding to Fig. 8, certainly makes sense.

It was stated above that the two basic improvements of the PB model have been made so far. We have just described the HPB model in some more detail. Now, we will briefly explain the PBD model. The basic idea is that the harmonic potential energy has been replaced by the anharmonic one through

$$\frac{k}{2}(y_n - y_{n-1})^2 \Rightarrow \frac{k}{2}\left[1 + \rho\, \mathrm{e}^{-\alpha(y_n + y_{n-1})}\right](y_n - y_{n-1})^2, \tag{50}$$

where ρ and α are constants [45–50]. This expression can be viewed as a harmonic interaction with a variable coupling constant [51]. It was mentioned above that

the stacking interaction stabilizes the helix. The nonlinear term, comprising positive parameters α and ρ, is the stacking potential. Widely used values taken in the calculations are $\alpha = 0.35\,\mathring{\text{A}}^{-1}$ and $\rho = 0.5$ [49].

It was stated above that $y_n(t)$ is not temperature-dependent, but its mean value is. Figure 9 shows how the mean value $\langle y \rangle$ depends on temperature [46]. The authors compared the two cases within the potential given by Eq. (50), that is, $\alpha = 0$ (PB model) and $\alpha \neq 0$ (PBD model). We see that $\langle y \rangle$ is slowly increasing function up to a certain temperature, when it sharply increases. This increase represents denaturation. In the case of the PBD model, denaturation is rather sharp and occurs at lower temperatures. It would be interesting to study temperature dependences of $\langle y \rangle$ relying on the HPB, as well as other models, which could be a future task. We want to point out that the temperature dependence of $\langle y \rangle$ also depends on the remaining parameters existing in the model, like D and a, describing the Morse potential.

The models explained above assume a homogeneous DNA chain, which might not be quite correct. For example, adenine and thymine are connected by double hydrogen bonds and guanine and cytosine by triple ones. Hence, one can expect that the corresponding Morse potential depths are D and $1.5D$. A crucial question is whether the wave characteristics, like amplitude, velocity, etc., drastically change whenever the wave reaches a new type of nucleotide pair. If so, the soliton would not be stable. It was explained that the breathers are not substantially affected by spatial inhomogeneities of the DNA sequence, but the kinks are [18]. This is in good agreement with the result explained in [52].

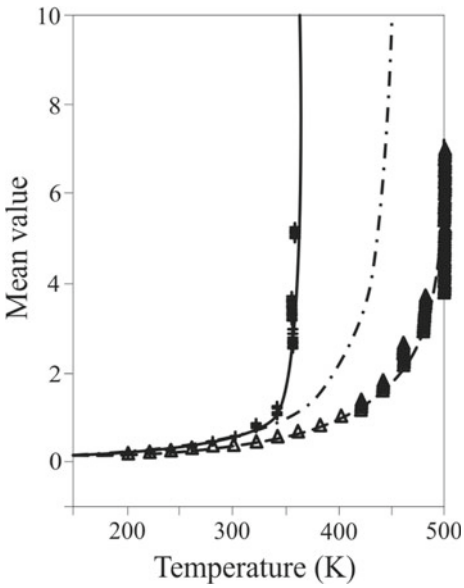

Fig. 9 Variation of the mean value $\langle y \rangle$ versus temperature for: $k = 0.04\ \text{eV}/\mathring{\text{A}}^2$, $a = 4.45\,\mathring{\text{A}}^{-1}$, and $D = 0.04$ eV. The solid line corresponds to the anharmonic stacking interaction ($\alpha = 0.35\ \mathring{\text{A}}^{-1}$, $\rho = 0.5$). The dashed and dash-dotted lines correspond to two cases ($\rho = 0.5$ and $\rho = 0$) of harmonic stacking interactions ($\alpha = 0$), respectively

2 Resonance Mode and DNA Opening

Any model can be considered good if it can explain something or predict a possible experiment. In this section, we show how the HPB model can explain a local opening of DNA, a well-known fact that happens during transcription. Let us study the functions $\omega_{\mathrm{o}}(ql)$ and $\omega_{\mathrm{a}}(ql)$, given by Eqs. (32) and (34), respectively. They also depend on the parameters k,K, a, and$D$, and, in general, are not equal. These frequencies were compared [33, 53], and it was speculated that their equality could represent a resonance mode (RM) [53]. Let us study this idea in some more detail. From Eqs. (32) and (34), one obtains

$$\omega_{\mathrm{o}}^2 - \omega_{\mathrm{a}}^2 \propto \frac{a^2 D}{K} + \cos(5ql), \tag{51}$$

as we are using $h = 5$ throughout this chapter. We easily recognize the following three possibilities:

$$(1)\ a^2 D > K \Rightarrow \omega_0 > \omega_{\mathrm{a}} \quad \text{for} \quad \forall ql, \tag{52a}$$

$$(2)\ a^2 D < K \Rightarrow \omega_0 < \omega_{\mathrm{a}} \text{ in some intervals of } ql, \tag{52b}$$

$$(3)\ a^2 D = K \Rightarrow \omega_0 = \omega_{\mathrm{a}} \quad \text{at } ql = \pi/5. \tag{52c}$$

Of course, there are other values for ql satisfying the requirement $\omega_{\mathrm{o}} = \omega_{\mathrm{a}}$, but they are not relevant now. The last case, i.e., Eq. (52c), corresponds to the RM, mentioned above [53]. The idea was further developed in [54, 55]. It was shown that some conditions yield very high amplitude [54]. Of course, the large amplitude does not necessarily mean the RM, and this behaviour was called extremely high amplitude (EHA) mode in [54]. However, some arguments in favour of RM were given in [55] and, in this chapter, the term RM will be used.

Problem 23 Return to Problem 11 and check on Eqs. (52a)–(52c).

Before we proceed, we want to discuss one important point. Equations (17) and (18) represent two decoupled equations of motion. How about the corresponding frequencies, given by Eqs. (32) and (34)? We should notice that ω_{o} and ω_a are not decoupled in the sense that they can be changed independently as both frequencies depend on the same parameters k and K. Hence, they are coupled through the common parameters [54]. In other words, we can eliminate one of these parameters and express ω_{o} as a function of ω_a, or vice versa. An example of such a function is Eq. (51).

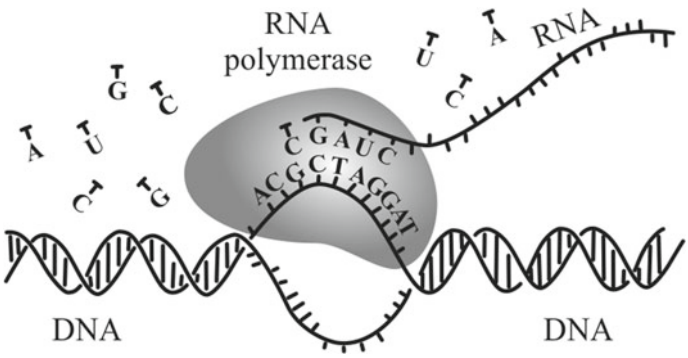

Fig. 10 Transcription of RNA

In what follows, we explain how the RM can explain the local opening of the DNA chain during the mRNA formation. The DNA–RNA transcription is nothing but the formation of mRNA molecule from RNA polymerase molecules (RNAP), as shown in Fig. 10 [5, 56]. Therefore, this occurs at the segments where the DNA chain is surrounded by the RNAP. We can call them transcription segments (TS). The transcription can be done only through active interaction between DNA and its surrounding. Let us imagine a segment of a single DNA strand. The nucleotides belonging to this strand can interact with the surrounding nucleotides only if they do not interact strongly with the remaining strand, which can be seen in Fig. 10. This means that the DNA chain should open locally, and this is what really happens during the transcription.

It was explained above that the mentioned parameters describe chemical bonds. This means that, due to the presence of RNAP, the interaction between the nucleotides belonging to the same pair is changed. In other words, the Morse potential at TSs is different from the potential at the rest of the molecule, which means that the RNAP transforms the Morse potential so that it becomes wider and shallower. This change could correspond to the transition from the blue to red cases in Fig. 2. Notice that the result of the local opening is the decrease in the value of the parameter K. Therefore, the RNAP interacts with the DNA nucleotides, decreasing the force between the different strands. This means that both K and a^2D go down, a^2D decreases faster, and, finally, the EHA vibrations occur ($K = a^2D$), which results in very large amplitude, i.e., in the local opening of the DNA chain.

It is worth mentioning that the decrease in the value of the parameter K might be an indication that the helicoidal interaction term in Eq. (16) is not linear. In other words, it might make sense to replace this term with the nonlinear one. This has not been done so far but should be one of the future tasks.

One can argue that $K = a^2D$ is not a sufficient condition for EHA vibrations, i.e., for the RM, as $ql = \pi/5$ is required in addition. However, it was explained above that $ql = \pi/5$ is probably the most favourable value, as indicated in Eq. (49). This is nothing but $N = 10$ in Fig. 8, which was explained previously.

The reader might have noticed that the optical frequency is Ω, given by Eq. (44), rather than ω_o. This is correct, but the simplified analysis has been quite appropriate till now to understand the idea. Therefore, a more correct requirement for the RM is

$$\Omega \equiv \omega_0 + \Delta\omega = \omega_a, \tag{53}$$

while $\omega_o = \omega_a$ represents its approximation. Of course, the expression for $\Delta\omega$ is determined by Eq. (44).

Till now, we have discussed the local opening and RM, but there was nothing that could be considered as possible proof of the real existence of the RM. The best and easiest thing that can be done is to study the amplitude existing in Eq. (42). We should investigate if it really goes to infinity under the mentioned conditions. It is convenient to introduce a positive dimensionless parameter p defined through

$$a = p\sqrt{K/D}. \tag{54}$$

Of course, the cases $p > 1, p < 1$, and $p = 1$ correspond to Eqs. (52a–c), respectively.

Figure 11 shows the amplitude as a function of the parameter p for three values of D. It was plotted according to Eqs. (21), (32), (33), (35), (36), (39), (43), and (46). Of course, the chosen values for D and K are smaller than the non-resonant ones used for Fig. 8. We can see that the amplitude really tends to infinity for a certain critical value of p. This is smaller than one due to the definition (53).

Two examples of the resonance solitons $y(n)$ are shown in Figs. 12 and 13. These functions were plotted like Fig. 8, but a was determined according to Eq. (54). It was explained above that the RM values of the parameters K and $a^2 D$ are smaller than the ordinary values, and we picked $K = 0.05$ N/m and $D = 0.05$ eV. Both figures were carried out for $t = 100$ ps. It is important to point out that the interaction between

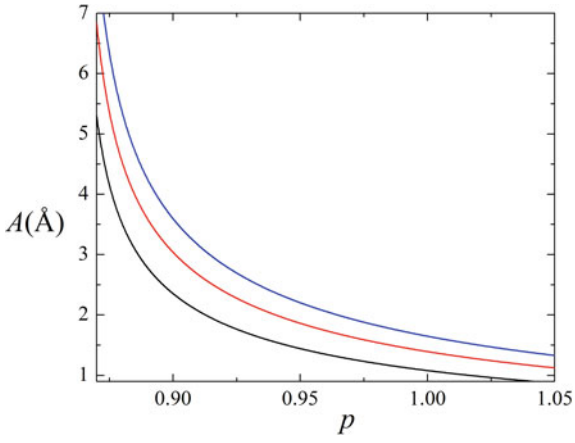

Fig. 11 Amplitude A as a function of p for $k = 12$ N/m, $K = 0.05$ N/m, $\eta = 0.47$ and $D = 0.07$ eV (blue), $D = 0.05$ eV (red), and $D = 0.03$ eV (black)

the RNAP and the corresponding DNA nucleotides does not affect the longitudinal interaction of the neighbouring nucleotides. Hence, the parameter k is not changed at those segments unlike K, a, and D. Notice that k does not appear in Eq. (54). Of course, the very high amplitude should not bother us as viscosity has been neglected.

It was explained why the positive amplitude in Fig. 8 is slightly bigger than the negative one. However, for the RM, the negative amplitude becomes negligible in comparison with the positive one. This is consistent with our attempt to describe the local opening of the DNA molecule.

It is very important to understand that the resonance cannot happen for $K = 0$. This means that the helicoidal structure provides the resonance, which shows the advantage of the HPB model over the PB one, which could be obtained from the HBD by letting $K = 0$. There is one more way to demonstrate this advantage. Figure 6 shows how modulation, i.e., the density of internal oscillations Γ_o, depends

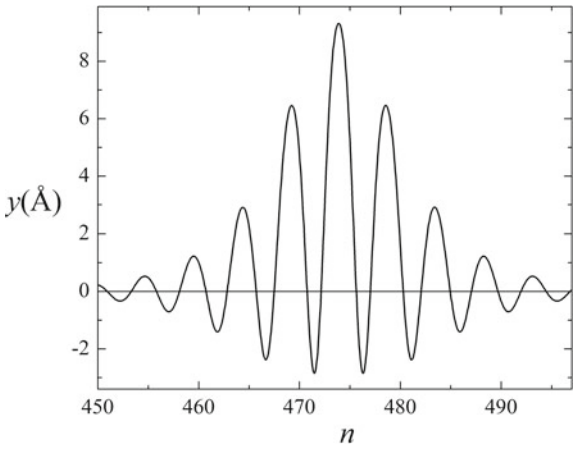

Fig. 12 Nucleotide pair stretching at $t = 100$ps for: $D = 0.05$ eV, $k = 12$ N/m, $K = 0.05$ N/m, $ql = 2\pi/10$, $\eta = 0.47$, and $p = 0.9$

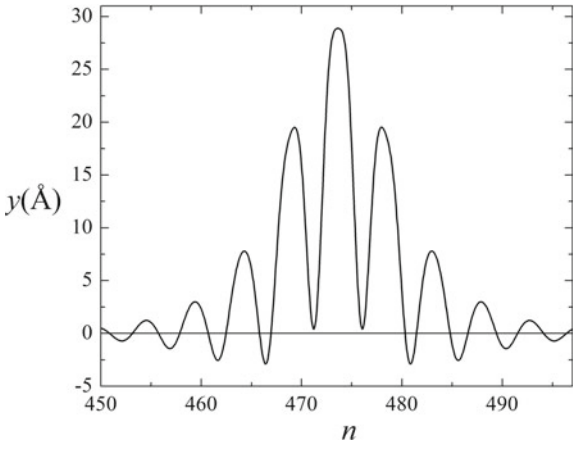

Fig. 13 Nucleotide pair stretching at $t = 100$ ps for: $D = 0.05$ eV, $k = 12$ N/m, $K = 0.05$ N/m, $ql = 2\pi/10$, $\eta = 0.47$, and $p = 0.87$

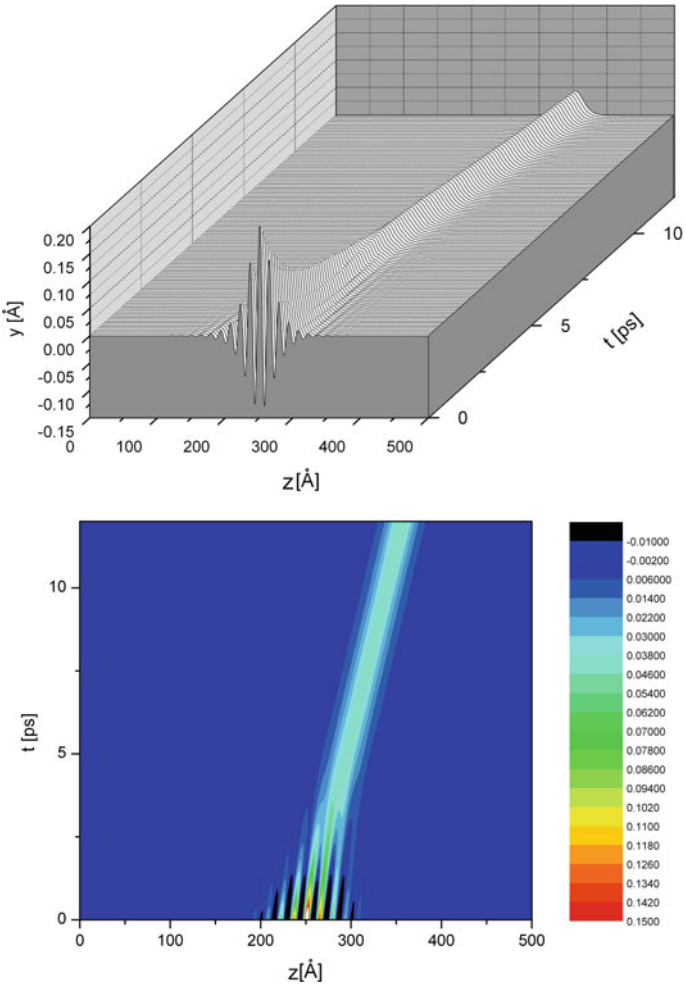

Fig. 14 Stretching of the nucleotide pair as a function of time and position for $g = 0.3$. (Reproduced with permission from [73])

on η for the particular K. We could have assumed a fixed value for η and plotted the function $\Gamma_o(K)$. This is an increasing function, showing that the higher K provides more efficient modulation.

Problem 24 Plot the function $\Gamma_o(K)$ for the parameters given by Eq. (49) and $\eta = 0.47$. Calculate Γ_o for $K = 0.08$ N/m. Compare with Problem 22. Notice the value of Γ_o for $K = 0$.

Let us study the soliton depicted in Fig. 13. According to Eq. (47), its width, in units of l, is $\Lambda_n \equiv \Lambda/l \approx 38$. However, the local opening can be related to its positive value only. We see that this relevant width is about 13 nucleotides. This can be compared with the experimental values, where the transcription bubble and RNA:DNA hybrid were reported to be 17 and 8 base pairs, respectively [43]. In [54], where slightly different values of the parameters were used, the agreement with these experimental values was almost perfect. However, we should not be too happy with providing such an agreement because, more or less, everything depends on a few parameters and, of course, different combinations of them can bring about an equal result.

A more detailed analysis of the RM exists in [54]. There, it was shown how the interval of the allowed values of K can be estimated. Also, the smallest value of p was calculated. Of course, this is the resonance value p_{R}. For the values of the parameters used in this paragraph, p_{R} is slightly smaller than 0.87, used for Fig. 13.

Figure 11 shows that the amplitude reaches extremely high values under certain conditions. However, each big amplitude does not necessarily mean RM. In the context of classical mechanics, the vibrations of an undamped linear oscillator, characterized by intrinsic frequency ω_i, when subjected under the action of the external harmonic force of frequency ω_f, must attain a resonance regime when $\omega_i = \omega_f$. How about the DNA molecule? Let us imagine an arbitrary nucleotide pair. If this pair was independent, i.e., free from any external influence, the centre of its mass would not move. This means that there would be only one mode, and these are out-of-phase oscillations. Therefore, the frequency ω_{o}, given by Eq. (32), corresponds to the intrinsic frequency ω_i of the classical undamped oscillator. However, when this nucleotide pair belongs to DNA, there is one more oscillating mode and the frequency ω_{a}. In other words, there is surrounding, which brings about one more mode. From the point of view of the nucleotide pair, this surrounding, i.e., the rest of DNA, is nothing but the external force [55]. Hence, we can expect the resonance mode to happen if these frequencies are equal as the friction is neglected and this is what we have stated in the paper. Therefore, the frequencies ω_{o} and ω_{a} correspond to the frequencies ω_i and ω_f, respectively [55].

At the beginning of this chapter, a couple of very important and relevant years were mentioned. Now, let us remember one more. This is 1992 when the first mechanical manipulation on a single molecule was performed [57]. Therefore, it is possible to stretch, wind, unwind, and so on, the single molecule [58–69]. The first molecule that was picked for such experiments was DNA [57]. There have been some suggestions for the experiments that would test the theory explained in this section [70]. It is very likely that such experiments are still not realistic to be performed. However, the value of the parameter k can be determined, as was suggested recently [71]. The idea for the experiment is based on the fact that the longitudinally applied force on DNA is proportional, in a rather big interval, to its extension [71]. It is important to point out that this linearity represents proof that the longitudinal interaction along with DNA [the second term in Eq. (13)] is properly modelled by the harmonic potential. Of course, if we knew the value of k, we would be able to estimate the remaining parameters better.

It was mentioned above that the very high amplitude should not bother us because viscosity has been neglected so far. Otherwise, the infinitely large amplitude would represent the destruction of the molecule. To provide a more realistic DNA model, we should take viscosity into consideration. This can be done by adding a viscous force

$$F_v = -\gamma\, \dot{y}_n \tag{55}$$

into Eq. (18), where γ represents a damping coefficient [72–74]. Following the same procedure as above, we obtain Eq. (35) again, while Eq. (36) becomes

$$F_2 = \delta_\gamma\, F_1^2; \quad \delta_\gamma = \omega_g^2\, \alpha \left[4\omega_\gamma^2 - \Delta + i4\chi\omega_\gamma\right]^{-1}, \tag{56}$$

where i is the imaginary unit and

$$\chi = \gamma \big/ 2m, \quad \omega_\gamma = -i\,\chi + \sqrt{\omega^2 - \chi^2}. \tag{57}$$

Hence, the optical frequency turns out to be complex now. In what follows, the index γ denotes the terms depending on the damping coefficient γ. NLSE holds again, where the dispersion and nonlinear parameters are

$$P_\gamma = \frac{1}{2\sqrt{\omega^2 - \chi^2}} \left\{ \frac{l^2}{m} \left[k\cos(ql) - K\,h^2\cos(qhl)\right] - V_\gamma^2 \right\} \tag{58}$$

and

$$Q_\gamma = -\frac{\omega_g^2}{2\sqrt{\omega^2 - \chi^2}} \left[2\alpha\,(\mu + \delta_\gamma) + 3\beta\right]. \tag{59}$$

Problem 25 Derive Eqs. (56) and (57) and show that the group velocity is $V_\gamma = \frac{\omega V_g}{\sqrt{\omega^2 - \chi^2}}$.

Problem 26 Derive the expression for Δ in Eq. (56).

(Solution: $\Delta = (4/m)\left[k\,\sin^2(ql)) + K\,\cos^2(qhl)\right] + \omega_g^2$).

Problem 27 Use the coordinate $S \equiv S_\gamma = Z - V_\gamma T$ instead of Eq. (37) and show that Eq. (38) holds again. Derive Eqs. (58) and (59).

A crucial point is the fact that the complex optical frequency yields to the complex Q, i.e.,

$$Q_\gamma = -\frac{\omega_g^2 \alpha}{\sqrt{\omega^2 - \chi^2}}(Q_1 + i\,Q_2) \equiv Q_r + i\,Q_i, \tag{60}$$

where

$$Q_1 = \mu + CM + 1.5\frac{\beta}{\alpha}, \quad Q_2 = CN, \quad C = \frac{\omega_g^2 \alpha}{M^2 + N^2} \tag{61}$$

$$M = 4(\omega^2 - \chi^2) - \Delta, \quad N = \frac{2\gamma}{m}\sqrt{\omega^2 - \chi^2}. \tag{62}$$

This means that Eq. (38) cannot be solved analytically anymore. A numerical solution is shown in Fig. 14 for $g = 0.3$, where

$$\gamma = g \times 10^{-11}\frac{\text{kg}}{\text{s}}. \tag{63}$$

We recognize the breather shown in Fig. 8. At a certain moment, denoted as zero in the figure, viscosity was introduced and the obtained wave looks like the envelope of the soliton in Fig. 8 with a smaller amplitude. This means that viscosity destroys modulation and the wave is a bell-type soliton. This is a very interesting result, having important biological implications, which will be explained later in more detail. It suffices now to state that the demodulation ensures long-lasting interaction between DNA nucleotides and RNAP, which is biologically very convenient [74].

Problem 28 Derive Eqs. (60)–(62).

Problem 29 Show that the requirement $P_\gamma > 0$ imposes $0 < g < 0.372$.

3 Demodulated Standing Solitary Wave and DNA–RNA Transcription

In this section, we study DNA:RNA transcription again. Hence, we keep in mind a certain TS and Fig. 10. However, instead of the RM, we study the transcription in the context of two new ideas. We rely on the HPB model again and follow [71].

Let us concentrate on a particular DNA nucleotide in Fig. 10. If this is an adenine, for example, it is bonded with DNA thymine, belonging to the other strand, but it also interacts with RNAP. Of course, the final positioning of RNA nucleotides should be a copy of the DNA segment. This obviously means that our DNA adenine should attract a certain RNA uracil and repel the remaining RNA nucleotides. This can be efficiently done only if the DNA adenine is far enough from its DNA partner during the transcription. Of course, this is really the case due to the local opening, as explained above.

Now, we go further in this direction of thinking. The local opening is certainly a necessary but not sufficient condition for successful transcription. The stretching of DNA, i.e., the distance between the DNA nucleotides belonging to the same pair, is described by Eq. (42). This certainly means that our adenine and thymine are far from each other during short periods of time only, and the adenine we have in mind does not have enough time to attract one RNA uracile. We do believe that the carrier wave is crucial for soliton movement through the DNA chain but is redundant when transcription occurs. Also, it is clear that only the envelope of Eq. (42) may correspond to the local opening. All this suggests the idea that the breather, moving along the chain, should be demodulated when it reaches the TSs. A mathematical interpretation of this requirement is

$$\Theta = 0, \qquad \Omega = 0, \tag{64}$$

as can be concluded according to Eq. (42). A crucial question is how demodulation happens at these segments. Our explanation is, like above, that RNAP changes the chemical milieu of DNA nucleotides, i.e., the values of relevant parameters, especially D and a, which yields to the values accommodating Eq. (64).

Therefore, the lack of internal oscillations prolongs the interaction between our adenine and uracil, but the question is whether this is enough for successful transcription. We should keep in mind that RNAP, during transcription, normally processes up to 100 bps per second [5]. This corresponds to propagation velocities of 34 nm/s, which is negligibly small in comparison with soliton velocities in DNA. Hence, a biologically convenient soliton is the one that is as slow as possible at TSs, as this would decrease the probability of genetic mistakes as much as possible. If we assume that nature has chosen genetically the best mode, then we may propose the idea that the soliton wave becomes a standing one at TSs. By the standing wave, we assume the one whose envelope velocity is equal to the RNAP velocity. As the latter one is negligible, we state [71]

$$V_e = 0. \tag{65}$$

Thus, Eqs. (64) and (65) provide food for thought, and, therefore, must be carefully checked. We here perform a mathematical analysis of the demodulated standing soliton (DSS) mode. This means that we investigate if there exists a certain value of ql that satisfies these equations. To simplify the mathematics, we introduce new parameters x, b, and s defined through the relations

$$K = x\,k, \quad b = 1 - \eta, \quad a^2 D = sk \tag{66}$$

and use $h = 5$, as explained earlier. As the parameter k determines the strong covalent bond, we know that both x and s should be much less than one.

It is convenient to introduce the following expressions:

$$\left.\begin{aligned} f_1 \equiv f_1(ql) &= \sin(ql) - 5x\sin(5ql) \\ f_2 \equiv f_2(ql) &= \cos(ql) - 25x\cos(5ql) \\ f_3 \equiv f_3(ql) &= \sin^2(ql/2) + x\cos^2(5ql/2) \end{aligned}\right\}. \tag{67}$$

Hence, the expression

$$V_g = \frac{kl}{m\omega} f_1 \tag{68}$$

is obvious, while Eqs. (44), (64), and (65) bring about useful formulas

$$V_g = 2P\frac{ql}{l}, \quad V_g(1-\eta) = \frac{\omega l}{ql} \tag{69}$$

Problem 30 Derive Eq. (69).

The next step is to solve the system (68), (39), and (69). Of course, Eqs. (66) and (67) should be applied. If we eliminate P and V_g, we straightforwardly obtain

$$b \equiv b(ql) = \frac{f_1}{qlf_2 - f_1}, \quad M_o \equiv \frac{m\omega^2}{k} = \frac{qlf_1^2}{qlf_2 - f_1}, \quad P = \frac{kl^2 f_1}{2qlm\omega}. \tag{70}$$

Problem 31 Derive Eq. (70).

Notice that the expression for P is simpler than the corresponding one in [71], although both are correct. Finally, Eqs. (32), (66), and (70) yield to

$$s \equiv s(ql) = \frac{ql\, f_1^2}{4(ql\, f_2 - f_1)} - f_3. \tag{71}$$

Also, according to Eqs. (21), (35), (36), (39), and (66), we easily obtain

$$\mu = -\frac{2\alpha s}{s+x}, \quad \delta = \frac{\alpha s}{M_0 - f_4 - s} \equiv \frac{\alpha s}{\delta_\mathrm{d}}, \tag{72}$$

$$Q = -\frac{2s^2k^2}{m\omega D}\Phi, \quad \Phi \equiv \Phi(ql) = \frac{7x - 11s}{s+x} + \frac{9s}{\delta_\mathrm{d}}, \tag{73}$$

where

$$f_4 \equiv f_4(ql) = \sin^2(ql) + x\cos^2(5ql). \tag{74}$$

It was mentioned above that we are looking for possible value(s) of ql that satisfy a couple of requirements. It is convenient to assume the wavelength as an integer of l, i.e.,

$$ql = \frac{2\pi}{\lambda}l = \frac{2\pi}{N}. \tag{75}$$

In the examples used for Figs. 8, 12, and 13, this integer was $N = 10$. If we assume that N cannot be smaller than six, then ql should be less than one. Therefore, the big values for ql are not acceptable. This means that f_1, existing in Eq. (67), is positive. In fact, it can be negative, but only for an unacceptable large x. As $f_1 > 0$ for any small enough ql, we conclude that $P > 0$ as well, which can be seen from Eq. (70).

There are a couple of requirements that should be satisfied. They are $b > 0.5$, $s > 0$, $\delta_\mathrm{d} \neq 0$, and $\Phi < 0$. The last one comes from Eq. (73), as the parameter Q should be positive to satisfy the requirement $PQ > 0$, as explained above. Let us take b as an example. Figure 15 shows $b(ql)$ for two values of x. We see that there should be

$$\left.\begin{array}{c} 0.25 < ql < 0.81 \quad \text{for} \quad x = 1/50 \\ ql < 0.77 \quad \text{for} \quad x = 1/80 \end{array}\right\}. \tag{76}$$

The part $ql > 0.25$ comes from the figure $s(ql)$. Also, $\delta_\mathrm{d} > 0$ for ql below the upper limits indicated in Eq. (76).

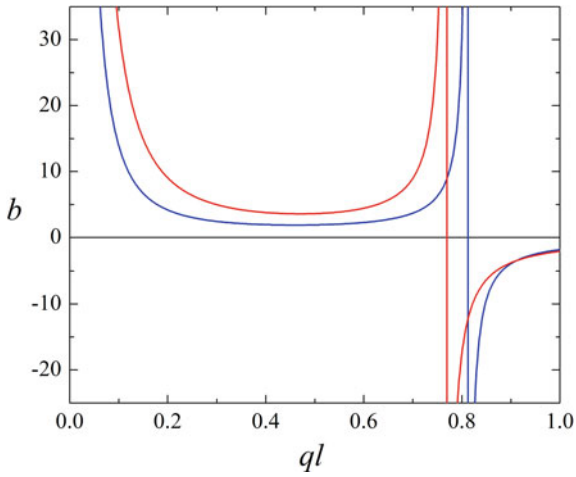

Fig. 15 Parameter b as a function of ql for: $x = 1/50$ (blue) and $x = 1/80$ (red)

Problem 32 Plot the figure $\delta_d(ql)$ and verify the statement in the previous sentence.

Problem 33 Plot the figure $s(ql)$ and determine the smallest value for ql.

The next step is the function $\Phi(ql)$, existing in Eq. (73). It is shown in Fig. 16. The only conclusion is

$$ql > 0.45 \quad \text{for} \quad x = 1/50. \tag{77}$$

Of course, the final allowed intervals for ql are given by Eqs. (76) and (77).

Therefore, there exist the values for ql satisfying the requirements for the DSS mode, i.e., Eqs. (64) and (65). Our final task is to plot the nucleotide pair stretching corresponding to the DSS mode. As an example, we pick $ql = 0.47$ rad and $x = 1/50$. For $D = 0.07$ eV and $k = 12$ N/m, from Eqs. (43) and (47), we easily calculate $A = 6.1$ Å, $\Lambda = 8l$, and $s = 0.03$. The second value means that the wave covers 8 base pairs, which perfectly matches the experimental value for the extent of the DNA:RNA hybrid [43]. This soliton is shown in Fig. 17 (blue), together with another example $ql = 0.20$ rad and $x = 1/80$, which yields to $A = 1.6$ Å, $\Lambda = 7.6l$, and $s = 0.05$ (red). The figure obviously shows the demodulated solitons. These are nothing but a kind of bell-type solitons. The big amplitudes are in agreement with the local opening of the chain.

Therefore, we demonstrated that ql satisfying our postulates explained above exists. Importantly, for the acceptable values of the relevant parameters, the corresponding soliton width matches the experimental value.

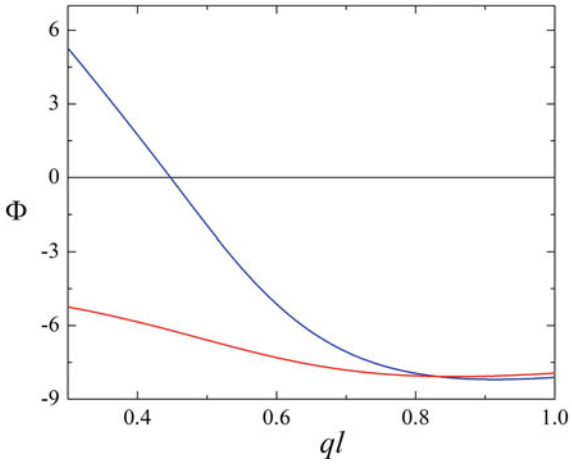

Fig. 16 Function $\Phi(ql)$ for: $x = 1/50$ (blue) and $x = 1/80$ (red)

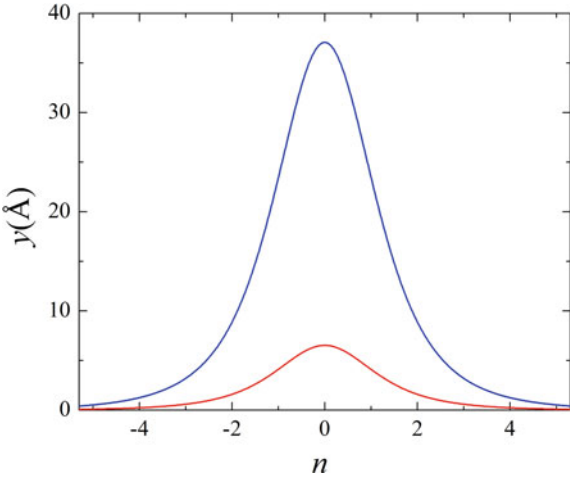

Fig. 17 Demodulated solitary waves for: $ql = 0.47$ rad, $x = 1/50$ (blue) and $ql = 0.20$ rad, $x = 1/80$ (red)

We complete this chapter with a couple of concluding remarks. We have dealt with DNA modelling. Two models, the Y and HPB, are explained in some more detail. They are examples of the angular and radial models, respectively. There have been a variety of attempts to improve these models, such as the model representing a combination of the Englander's and PB models, which brings about the kink soliton [75].

Let us compare the models explained in the first part of Sect. 1 with the HPB one. A reader might come to the conclusion that the first group of them may yield towards the kink-type solitons, while the HPB is reserved for the breathers. However, this would not be quite correct. Within the HPB model, the semi-discrete approximation has been applied. It has turned out that, according to this mathematical procedure, the breathers move along the chain. However, the continuum approximation can be used

as well, which yields the kinks moving along the chain [76]. Besides the kinks, the bell-type solitons were obtained in the case of negligible viscosity. Therefore, the final result does not depend on the studied system only, but on the applied mathematics as well. Of course, a crucial question is which of these solitons really exist in DNA, if any. It was argued that kinks and breathers do not exclude each other and that both solitons play an important role in DNA functioning [76]. Let us keep in mind the DNA–RNA transcription again. From the point of view of a single nucleotide pair, two nucleotides oscillate in a transverse direction around a certain distance. If this distance is large, then the local opening will more likely happen. The kink certainly means a certain step, which can be an increase in the distance around which the nucleotides oscillate. If so, then the kink could be understood as a prerequisite for the breather [76]. Regarding the mathematical methods, it is worth mentioning the method based on Jacobi elliptic functions [77] and fractional Lagrange formalism [78, 79]. They yield to the breathers again, i.e., to the results obtained using the semi-discrete approximation and shown above.

It was pointed out that the prerequisite for DNA–RNA transcription is the local opening. However, it is known that DNA must also unwind locally to let one strand serve as a template for the synthesis of a new strand of RNA [5]. The HPB model can take this into consideration. Namely, the local angle of helix winding is defined by the value of the parameter h. The partially unwinding chain corresponds to the decrease of h. We have been dealing with constant h so far. However, possible generalization, i.e., allowing it to be a variable at TSs, could be a topic of further research.

It might be important to point out that thermodynamics of local DNA opening was studied in [79], relying on the PB model. One of the future research tasks should be an extension of this work. This means that the HPB model should be used instead of its simpler predecessor. The HPB model is doubtlessly better than the PB one, and its advantage is especially important when we study the local opening. Namely, the term comprising K is extremely important as it describes the helicoidal structure of DNA.

A patient reader has certainly noticed that the big amplitudes are not in agreement with the earlier assumptions of small oscillations. This means that the HPB model only predicts the RM and DSS modes but is not adequate for complete quantitative analysis.

Let us complete this section with a few more words about the HPB model. The RM and DSS modes have been studied neglecting viscosity. The introduction of the dumping effects would be an important advantage, but a real challenge as well. Also, these two modes have been studied independently. One of the future tasks should be an attempt to involve both of them in a single theory. It is clear that DNA modelling has made tremendous progress during the past couple of decades. However, the velocity of increasing the volume of knowledge cannot match the velocity of appearing new questions. This means that the life of a biophysicist working on this topic is very interesting.

Acknowledgements The author would like to acknowledge the contribution of the COST Action CA17139. The author also acknowledges support from Project within the Cooperation Agreement between the JINR, Dubna, Russian Federation, and Ministry of Education, Science and Technological Development of the Republic of Serbia: Theory of Condensed Matter Physics.

References

1. J.D. Watson, F.H. Crick, Nature **171**, 737 (1953)
2. J.D. Watson, *Molecular Biology of the Gene* (W.A. Benjamin INC., Menlo Park, California, USA, 1976)
3. M.V. Volkenstein, *Biofizika* (Nauka, Moscow, 1981). (in Russian)
4. B. Alberts, D. Bray, J. Lewis, M. Raff, K. Roberts, J.D. Watson, *Molecular Biology of the Cell* (Garland Publishing Inc., New York, London, 1994)
5. C.R. Calladine, H.R. Drew, F.B. Luisi, A.A. Travers, *Understanding DNA* (Elsevier Academic Press, 2004)
6. S. Zdravković, In *Finely Dispersed Particles: Micro-, Nano-, and Atto-Engineering*, ed. by A.M. Spasic and J.P. Hsu (130 Surfactant Science Series, Dekker/CRC Press/Taylor & Francis Group, Boca Raton, Florida, 2006), p. 779
7. S. Zdravković, J. Nonlin. Math. Phys. **18**(Suppl. 2), 463 (2011)
8. M. Peyrard, Nonlinearity **17**, R1 (2004)
9. L.V. Yakushevich, *Nonlinear Physics of DNA* (Wiley Series in Nonlinear Science, Wiley, Chichester, 1998)
10. S.W. Englander, N.R. Kallenbach, A.J. Heeger, J.A. Krumhansl, S. Litwin, P. Natl, Acad. Sci. USA **77**, 7222 (1980)
11. M. Lakshmanan, S. Rajasekar, *Nonlinear Dynamics* (Springer, India, 2009)
12. A. Scott, *Nonlinear Science, Emergence and Dynamics of Coherent Structures* (Moscow, Russia, 2007. (in Russian)
13. M. Cadoni, R. De Leo, G. Gaeta, J. Phys. A: Math. Theor. **40**, 12917 (2007)
14. M. Cadoni, R. De Leo, G. Gaeta, J. Nonlin. Math. Phys. **14**, 128 (2007)
15. M. Cadoni, R. De Leo, S. Demelio, G. Gaeta, J. Nonlin. Math. Phys. **17**, 557 (2010)
16. L.V. Yakushevich, Phys. Lett. A **136**, 413 (1989)
17. G. Gaeta, Phys. Lett. A **143**, 227 (1990)
18. G. Gaeta, Phys. Lett. A **190**, 301 (1994)
19. G. Gaeta, Phys. Rev. E **74**, 021921 (2006)
20. M. Cadoni, R. De Leo, S. Demelio, J. Nonlin. Math. Phys. **18**, 287 (2011)
21. M. Cadoni, R. De Leo, G. Gaeta, Phys. Rev. E **75**, 021919 (2007)
22. F.K. Zakiryanov, L.V. Yakushevich, Comp. Res. Model. **5**, 821 (2013). (in Russian)
23. L.V. Yakushevich, V.N. Balashova, F.K. Zakiryanov, Matem. Biol. Bioinformatika **11**, 81 (2016). (in Russian)
24. G.F. Zhou, C.T. Zhang, Phys. Scripta **43**, 347 (1991)
25. M. Barbi, S. Cocco, M. Peyrard, Phys. Lett. A **253**, 358 (1999)
26. M. Barbi, S. Lepri, M. Peyrard, N. Theodorakopolous, Phys. Rev. E **68**, 061909 (2003)
27. G. Gaeta, L. Venier, Phys. Rev. E **78**, 011901 (2008)
28. G. Gaeta, L. Venier, J. Nonlin. Math. Phys. **15**, 186 (2008)
29. M. Cadoni, R. De Leo, S. Demelio, G. Gaeta, Int. J. Nonlin. Mech. **43**, 1094 (2009)
30. M. Peyrard, A.R. Bishop, Phys. Rev. Lett. **62**, 2755 (1989)
31. T. Dauxois, M. Peyrard, A.R. Bishop, Phys. Rev. E **47**, 684 (1993)
32. G. Gaeta, C. Reiss, M. Peyrard, T. Dauxois, Riv. Nuovo Cimento **17**, 1 (1994)
33. T. Dauxois, Phys. Lett. A **159**, 390 (1991)
34. T.R. Strick, M.N. Dessinges, G. Charvin, N.H. Dekker, J.F. Allemand, D. Bensimon, V. Croquette, Rep. Prog. Phys. **66**, 1 (2003)

35. T. Kawahara, J. Phys, Soc. Japan **35**, 1537 (1973)
36. R.K. Dodd, J.C. Eilbeck, J.D. Gibbon, H.C. Morris, *Solitons and Nonlinear Wave Equations* (Academic Press Inc., London, 1982)
37. M. Remoissenet, M. Peyrard, Phys. Rev. B **29**, 3153 (1984)
38. T. Dauxois, M. Peyrard, *Physics of Solitons* (Cambridge University Press, Cambridge, 2006)
39. A.C. Scott, F.Y.F. Chu, D.W. McLaughlin, Proc. IEEE **61**, 1443 (1973)
40. S. Zdravković, M.V. Satarić, Phys. Lett. A **373**, 126 (2008)
41. S. Zdravković, M.V. Satarić, Phys. Rev. E **73**, 021905 (2006)
42. S. Zdravković, M.V. Satarić, Phys. Lett. A **373**, 2739 (2009)
43. J. Gelles, R. Landick, Cell **93**, 13 (1998)
44. U. Siebenlist, Nature **279**, 651 (1979)
45. G. Weber, Europhys. Lett. **73**, 806 (2006)
46. T. Dauxois, M. Peyrard, A.R. Bishop, Phys. Rev. E **47**, R44 (1993)
47. T. Dauxois, M. Peyrard, Phys. Rev. E **51**, 4027 (1995)
48. D.X. Macedo, I. Guedes, E.L. Albuquerque, Phys. A **404**, 234 (2014)
49. M. Zoli, Eur. Phys. J. E **34**, 68 (2011)
50. T.S. van Erp, S. Cuesta-Lopez, M. Peyrard, Eur. Phys. J. E **20**, 421 (2006)
51. M. Peyrard, S. Cuesta-López, D. Angelov, J. Phys.-Condens. Mat. **21**, 034103 (2009)
52. S. Zdravković, M.V. Satarić, BioSystems **105**, 10 (2011)
53. S. Zdravković, M.V. Satarić, Chin. Phys. Lett. **22**, 850 (2005)
54. S. Zdravković, M.V. Satarić, Europhys. Lett. **78**, 38004 (2007)
55. S. Zdravković, M.V. Satarić, Europhys. Lett. **80**, 38003 (2007)
56. T. Lipniacki, Phys. Rev. E **60**, 7253 (1999)
57. S.B. Smith, L. Finzi, C. Bustamante, Science **258**, 1122 (1992)
58. G.U. Lee, L.A. Chrisey, R.J. Colton, Science **266**, 771 (1994)
59. S.B. Smith, Y. Cui, C. Bustamante, Science **271**, 795 (1996)
60. U. Bockelmann, B. Essevaz-Roulet, F. Heslot, Phys. Rev. E **58**, 2386 (1998)
61. T. Strunz, K. Oroszlan, R. Schäfer, H.-J. Güntherodt, Proc. Natl. Acad. Sci. USA **96**, 11277 (1999)
62. H. Clausen-Schaumann, M. Rief, C. Tolksdorf, H.E. Gaub, Biophys. J. **78**, 1997 (2000)
63. M.C. Williams, K. Pant, I. Rouzina, R.L. Karpel, Spectroscopy **18**, 203 (2004)
64. T. Lionnet, S. Joubaud, R. Lavery, D. Bensimon, V. Croquette, Phys. Rev. Lett. **96**, 178102 (2006)
65. J. Yan, T.J. Maresca, D. Skoko, C.D. Adams, B. Xiao, M.O. Christensen, R. Heald, J.F. Marko, Mol. Biol. Cell **18**, 464 (2007)
66. E.A. Galburt, S.W. Grill, C. Bustamante, Methods **48**, 323 (2009)
67. F. Mosconi, J.F. Allemand, D. Bensimon, V. Croquette, Phys. Rev. Lett. **102**, 078301 (2009)
68. C.P. McAndrew, C. Tyson, J. Zischkau, P. Mehl, P.L. Tuma, I.L. Pegg, A. Sarkar, Biotechniques **60**, 21 (2016)
69. R. Fabian Jr., C. Tyson, P.L. Tuma, I. Pegg, A. Sarkar, Micromachines **9**, 188 (2018)
70. S. Zdravković, M.V. Satarić, Phys. Lett. A **373**, 4453 (2009)
71. S. Zdravković, M.V. Satarić, A.Y.U. Parkhomenko, A.N. Bugay, Chaos **28**, 113103 (2018)
72. T. Das, S. Chakraborty, Europhys. Lett. **83**, 48003 (2008)
73. C.B. Tabi, A. Mohamadou, T.C. Kofané, Chin. Phys. Lett. **26**, 068703 (2009)
74. S. Zdravković, M.V. Satarić, Lj. Hadžievski, Chaos **20**, 043141 (2010)
75. D.L. Hien, N.T. Nhan, N.V. Thanh, N.A. Viet, Phys. Rev. E **76**, 021921 (2007)
76. S. Zdravković, D. Chevizovich, A.N. Bugay, A. Maluckov, Chaos **29**, 053118 (2019)
77. S. Zdravković, C.B. Tabi, J. Comput. Theor. Nanosc. **7**, 1418 (2010)
78. A. Mvogo, T.C. Kofané, Chaos **26**, 123120 (2016)
79. A. Mvogo, G.H. Ben-Bolie, T.C. Kofané, Commun. Nonlinear Sci. **48**, 258 (2017)
80. T. Lipniacki, Phys. Rev. E **64**, 051919 (2001)